Article

Intersystem Crossing versus Electron Transfer in Porphyrin-Based Donor–Bridge–Acceptor Systems: Influence of a Paramagnetic Species

Karin Pettersson, Kristine Kils, Jerker Mrtensson, and Bo Albinsson

J. Am. Chem. Soc., **2004**, 126 (21), 6710-6719• DOI: 10.1021/ja0370488 • Publication Date (Web): 11 May 2004

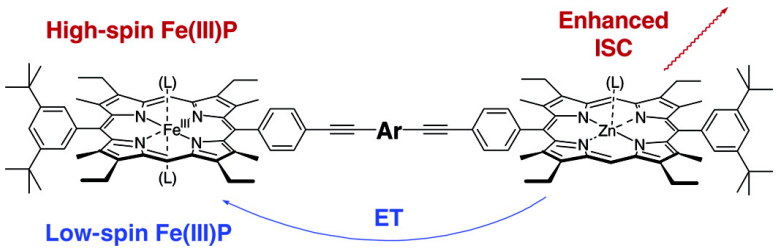

More About This Article

Additional resources and features associated with this article are available within the HTML version:

- Supporting Information
- Links to the 6 articles that cite this article, as of the time of this article download
- Access to high resolution figures
- Links to articles and content related to this article
- Copyright permission to reproduce figures and/or text from this article

View the Full Text HTML

J|A|C|S
ARTICLES
Published on Web 05/11/2004

Intersystem Crossing versus Electron Transfer in Porphyrin-Based Donor−Bridge−Acceptor Systems: Influence of a Paramagnetic Species

Karin Pettersson,[†] Kristine Kilså,[‡,§] Jerker Mårtensson,[†] and Bo Albinsson*,[†]

Contribution from the Department of Chemistry and Bioscience, Chalmers University of Technology, SE-412 96 Göteborg, Sweden, and Beckman Institute, MC 139-74, California Institute of Technology, Pasadena, California 91125

Received July 3, 2003; E-mail: balb@chembio.chalmers.se

Abstract: We have investigated how the spin state of an acceptor influences the photophysical processes in a donor−bridge−acceptor (D−B−A) system. The system of choice has zinc porphyrin as the electron donor and high- or low-spin iron(III) porphyrin as the acceptor. The spin state of the acceptor porphyrin is switched simply by coordinating imidazole ligands to the metal center. The D−A center−center distance is 26 Å, and the bridging chromophore varies from π-conjugated to a σ-bonded system. The presence of a high-spin iron(III) porphyrin in such systems has previously been shown to significantly enhance intersystem crossing in the remote zinc porphyrin donor, whereas no significant electron transfer to the iron porphyrin acceptor was observed, even though the thermodynamics would allow for photoinduced electron transfer. Here, we demonstrate that by switching the acceptor to a low-spin state, the dominating photophysical process is drastically changed; the low-spin system shows long-range electron transfer on the picosecond time-scale, and intersystem crossing occurs at its "normal" rate.

Introduction

Excitation energy transfer and photoinduced electron transfer are processes of great interest in many research areas. The most important energy- and electron-transfer processes occur in natural photosynthesis. Light-harvesting molecules transfer energy to the reaction center where a sequence of electron-transfer reactions takes place. Several research groups are trying to design systems capable of artificial photosynthesis. To achieve this, a detailed understanding of the energy and the electron-transfer processes is of considerable value. Also, for the development of molecular scale electronic components, such as switches, transistors, and rectifiers, etc., these processes are of great importance. Several review articles have been published on both of these subjects.[1−9]

The present study is part of an ongoing effort to investigate how the rate of energy and electron transfer could be modulated by the intervening medium.[10−14] When designing the donor−bridge−acceptor (D−B−A) systems with a high-spin iron(III) porphyrin as the acceptor (Figure 1), we initially expected electron transfer to be the dominating deactivation pathway for the lowest singlet excited state of the donor moiety.[14] It turned out, however, not to be the case. The singlet excited state of the donor was significantly quenched, but by an enhanced intersystem crossing process rather than electron transfer. The proximity between the donor porphyrin and the high-spin iron(III) porphyrin was suggested to be responsible for the enhanced intersystem crossing. The purpose of the present study is to investigate if the spin state of the paramagnetic iron(III) porphyrin influences the rate of the different deactivation processes, in particular electron transfer and donor intersystem crossing. In the iron(III) porphyrins, the spin state is sensitive to ligands that coordinate to the metal, and it has been suggested that Lewis base ligands such as imidazole induce a low-spin ($S = {}^1/_2$) electron configuration whereas a chloride ligand induces a high-spin ($S = {}^5/_2$) situation.[15]

The studied systems (Figure 1) consist of three separate chromophores: donor, bridge, and acceptor. The donor is a zinc(II) 5,15-diphenyl-2,8,12,18-tetraethyl-3,7,13,17-tetramethylporphyrin (ZnP). The corresponding acceptor porphyrin is either a high-spin iron(III) porphyrin (Fe(Cl)P) or a low-spin

[†] Chalmers University of Technology.
[‡] California Institute of Technology.
[§] Present address: Department of Physical Chemistry, Box 579, Uppsala University, SE-75123 Uppsala, Sweden.

(1) Speiser, S. *Chem. Rev.* **1996**, *96*, 1953−1976.
(2) Turro, N. J. *Pure Appl. Chem.* **1977**, *49*, 405−429.
(3) Ward, M. D. *Chem. Soc. Rev.* **1997**, *26*, 365−375.
(4) Closs, G. L.; Miller, J. R. *Science* **1988**, *240*, 440−447.
(5) Gust, D.; Moore, T. A.; Moore, A. L. *IEEE Eng. Med. Biol. Magn.* **1994**, *13*, 58−66.
(6) Wasielewski, M. R. *Chem. Rev.* **1992**, *92*, 435−461.
(7) Piotrowiak, P. *Chem. Soc. Rev.* **1999**, *28*, 143−150.
(8) Burrell, A. K.; Wasielewski, M. R. *J. Porphyrins Phthalocyanines* **2000**, *4*, 401−406.
(9) Anderson, H. L. *Chem. Commun.* **1999**, 2323−2330.
(10) Kilså, K.; Kajanus, J.; Mårtensson, J.; Albinsson, B. *J. Phys. Chem. B* **1999**, *103*, 7329−7339.
(11) Andréasson, J.; Kajanus, J.; Mårtensson, J.; Albinsson, B. *J. Am. Chem. Soc.* **2000**, *122*, 9844−9845.
(12) Andréasson, J.; Zetterqvist, H.; Kajanus, J.; Mårtensson, J.; Albinsson, B. *J. Phys. Chem. A* **2000**, *104*, 9307−9314.
(13) Kilså, K.; Kajanus, J.; Macpherson, A. N.; Mårtensson, J.; Albinsson, B. *J. Am. Chem. Soc.* **2001**, *123*, 3069−3080.
(14) Kilså, K.; Kajanus, J.; Larsson, S.; Macpherson, A. N.; Mårtensson, J.; Albinsson, B. *Chem.-Eur. J.* **2001**, *7*, 2122−2133.
(15) Scheidt, W. R.; Reed, C. A. *Chem. Rev.* **1981**, *81*, 543−555.

10.1021/ja0370488 CCC: $27.50

Low-spin complexes Zn(Im)P-RB-Fe(Im)$_2$P$^+$

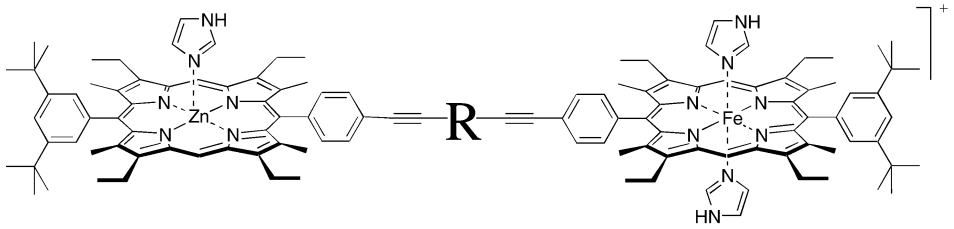

High-spin complexes ZnP-RB-Fe(Cl)P

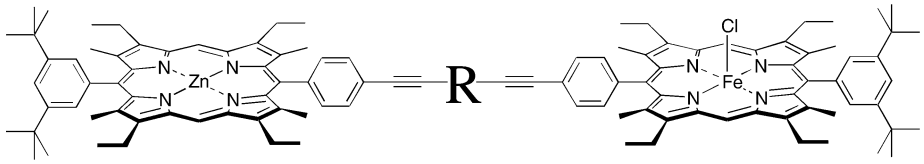

Bridging chromophores RB

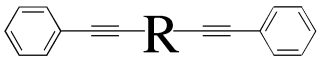

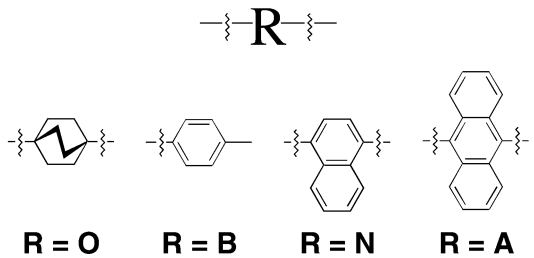

Figure 1. Structures of the low-spin iron(III) porphyrin, Zn(Im)P−RB−Fe(Im)$_2$P$^+$, the high-spin iron(III) porphyrin, ZnP−RB−Fe(Cl)P, and the bridges RB = OB, BB, NB, and AB.

iron(III) porphyrin (Fe(Im)$_2$P$^+$) with two imidazole ligands coordinated to the iron. Please note, when imidazole is present it also coordinates to the zinc porphyrin (Zn(Im)P), thus also altering the donor properties. The four bridging chromophores are 1,4-bis(phenylethynyl)bicyclo-octane (OB), 1,4-bis(phenylethynyl)benzene (BB), 1,4-bis(phenylethynyl)naphthalene (NB), and 9,10-bis(phenylethynyl)anthracene (AB). The methyl groups in the porphyrin β-positions cause sterical hindrance and force the porphyrin to be nearly perpendicular to the bridging chromophore, thus preventing the chromophores from being π-conjugated.

Studies on related donor−acceptor systems with zinc and iron(III) porphyrins have shown that electron transfer is the major deactivation route at short D−A distances.[16−22] For our ZnP−RB−Fe(Cl)P system (Figure 1), which all have a 26 Å D−A center-to-center distance, no electron transfer was observed. In lack of evidence for electron transfer, we have shown that enhanced intersystem crossing and energy transfer are the major deactivation routes.[14] Enhanced intersystem crossing in zinc or free base porphyrin donors linked to paramagnetic copper(II) porphyrins has also been observed by Aseno-Someda and co-workers.[23−25]

The present work focuses on the deactivation channels for the series of D−B−A systems with a low-spin Fe(Im)$_2$P$^+$ acceptor (Figure 1). Furthermore, the quenching properties of the D−B−A systems with a high-spin Fe(Cl)P are compared to those containing a low-spin Fe(Im)$_2$P$^+$ acceptor.

Experimental Section

Materials. The syntheses of the D−B−A systems as well as the relevant reference compounds D−B are described elsewhere.[10,14,26] All solvents − 2-methyl-tetrahydrofuran (2Me-THF), methylene chloride (CH_2Cl_2), *N*,*N*-dimethylformamide (DMF), chloroform ($CHCl_3$) − were

(16) Helms, A.; Heiler, D.; McLendon, G. *J. Am. Chem. Soc.* **1992**, *114*, 6227−6238.
(17) Osuka, A.; Tanabe, N.; Kawabata, S.; Yamazaki, I.; Nishimura, Y. *J. Org. Chem.* **1995**, *60*, 7177−7185.
(18) Osuka, A.; Maruyama, K.; Mataga, N.; Asahi, T.; Yamazaki, I.; Tamai, N. *J. Am. Chem. Soc.* **1990**, *112*, 4958−4959.
(19) Tamiaki, H.; Nomura, K.; Maruyama, K. *Bull. Chem. Soc. Jpn.* **1994**, *67*, 1863−1871.
(20) Portela, C. F.; Brunckova, J.; Richards, J. L.; Schollhorn, B.; Iamamoto, Y.; Magde, D.; Traylor, T. G.; Perrin, C. L. *J. Phys. Chem. A* **1999**, *103*, 10540−10552.
(21) Mataga, N.; Yao, H.; Okada, T.; Kanda, Y.; Harriman, A. *Chem. Phys.* **1989**, *131*, 473−480.
(22) de Rege, P. J. F.; Williams, S. A.; Therien, M. J. *Science* **1995**, *269*, 1409−1413.
(23) Asano-Someda, M.; Kaizu, Y. *Inorg. Chem.* **1999**, *38*, 2303−2311.
(24) Toyama, N.; Asano-Someda, M.; Ichino, T.; Kaizu, Y. *J. Phys. Chem. A* **2000**, *104*, 4857−4865.
(25) Asano-Someda, M.; Jinmon, A.; Toyama, N.; Kaizu, Y. *Inorg. Chim. Acta* **2001**, *324*, 347−351.
(26) Kilså, K.; Macpherson, A. N.; Gillbro, T.; Mårtensson, J.; Albinsson, B. *Spectrochim. Acta, Part A* **2001**, *57*, 2213−2227.

used as purchased. Imidazole (Im) was purchased from Fluka AG and used as received. To form the low-spin complexes, the high-spin complexes were dissolved in a solution containing imidazole in excess to ascertain full conversion to Zn(Im)P and $Fe(Im)_2P^+$ (vide infra).

Ground-state absorption spectroscopy was performed with a Cary 4 Bio spectrophotometer. The spectral bandwidth was 0.5 nm, and the scanning rate was 300 nm/min. Spectrophotometric titrations of FeP with imidazole were performed in $CHCl_3$, 2Me-THF, DMF, and CH_2Cl_2.

Steady-State Fluorescence Spectroscopy. The fully corrected emission spectra were recorded with a SPEX Fluorolog 3 or a SPEX Fluorolog $\tau 2$ spectrofluorimeter. The absorbance at the excitation wavelength was kept low, approximately 0.05 (corresponding to a concentration of approximately 2.5 μM), to avoid inner filter effects and intermolecular interactions. The systems were excited at the maximum of the donor Q-band absorption (545−555 nm, depending on solvent and coordinating species). Steady-state fluorescence measurements were performed in 2Me-THF, DMF, and CH_2Cl_2.

Time-resolved fluorescence spectroscopy was carried out using the time-correlated single photon counting (TCSPC) method. The excitation source was the second harmonic of a Ti:Sapphire oscillator (Tsunami, Spectra Physics), pumped by a continuous-wave frequency-doubled diode pumped Nd:YVO_4 laser (Millennia Vs, Spectra Physics). The photons were collected by a microchannel plate photomultiplier tube (MCP-PMT R3809U-50, Hamamatsu) and fed into a multichannel analyzer with 4096 channels yielding a time resolution of about 10 ps (fwhm). A diluted silica sol scattering solution was used to collect the instrument response signal. Further, the collected crude decay curves were iteratively convoluted and evaluated using the software package F900 (Edinburgh Instruments). The excitation wavelength was in the Soret band region (400−420 nm) for technical reasons. In all experiments, the absorption at the excitation wavelength was set to 0.1−0.4, and at least 10 000 photons were collected in the top channel within 5 min. Time-resolved fluorescence was performed in 2Me-THF, DMF, and CH_2Cl_2.

Nanosecond transient absorption kinetic traces were recorded by using the signal from an OPO (Surelite OPO, Continuum) pumped by a Nd:YAG laser (fwhm = 6 ns, Surelite II-10, Continuum). A xenon arc lamp was used as probe light source followed by a conventional monochromator photomultiplier system (symmetrical Czerny-Turner arrangements and a five-stage Hamamatsu R928). Data acquisition was performed via a Tektronix TDS 2022 digital oscilloscope interfaced to a PC-based A-D-card and averaged in a LabView program.

All samples were degassed either by bubbling argon gas for 10 minutes or by six freeze−pump−thaw cycles. The ground-state absorbance at the excitation wavelength was below 0.05, and 2Me-THF was used as solvent. The systems were excited at the maximum of the donor Q-band absorption (545−555 nm, depending on solvent and coordinating species). Further, the kinetic traces were collected at the maximum donor triplet−triplet absorption (470 nm for both ZnP and Zn(Im)P), and 64 decay traces were averaged to form the kinetic traces.

For femtosecond transient absorption measurements, the pump−probe technique was employed. The sample was excited at the Q-band maximum (545−555 nm, coordination dependent) with the second harmonic of the signal from a TOPAS (Light Conversion Ltd.). The TOPAS was pumped by a Ti:Sapphire regenerative amplifier (Spitfire, Spectra Physics) at 1 kHz repetition rate. The regenerative amplifier was pumped by a frequency-doubled diode-pumped Nd:YLF laser (Evolution-X, Spectra Physics) and seeded by a mode-locked femtosecond Ti:Sapphire laser (Tsunami, Spectra Physics). The seed laser was pumped by a continuous-wave frequency-doubled diode-pumped Nd:YVO_4 laser (Millennia Vs, Spectra Physics). Further, the output from the regenerative amplifier (~130 fs) was split into two beams with a beam splitter (70/30), the pump beam and the probe beam. The pump beam (the output from the TOPAS) was chopped at 500 Hz to block the pump every second pulse. Subsequently, the pump beam was sent through a computer-controlled optical delay line (Aerotech) and then focused with reflective optics on the sample at a small angle relative to the probe beam. The polarization of the pump beam relative to the polarization of the probe beam was set to the magic angle by a Berek compensator (New Focus), and the pulse energy at the sample in a typical experiment was 1.4 μJ/pulse. The intensity of the probe beam was reduced by two neutral density filters (one OD = 4 and one variable 0−2), before it was focused into a thin sapphire plate to generate a white light continuum. A second beam splitter (50/50) was used to split the generated white light continuum into the probe and the reference beams. Both beams were focused on the sample, with the probe beam overlapping the pump beam. After the sample, both probe and reference beams were focused onto the slit of a computer-controlled monochromator (ISA, TRIAX 180). Three photodiodes were used to monitor the intensity of probe, reference, and pump beams, respectively. The signals were gated by boxcar integrators (SR250, Stanford Research Systems), fed into a PC-based A-D-card, and averaged by a LabView program.

Transient absorption spectra were recorded at different delay times with a wavelength step of 2 nm and a monochromator bandwidth of 14 nm. Transient absorption decays were recorded at different wavelengths with a monochromator bandwidth of 14 nm. The sample was held in a static 1 mm path length cuvette, and the optical density at the excitation wavelength was approximately 1. The decay traces were fitted to a sum of exponentials with the Matlab software package. 2Me-THF was used as solvent.

Electron paramagnetic resonance (EPR) X-band spectra were measured on a Bruker EMX instrument with a standard TE_{102} cavity. In all experiments, the modulation amplitude was 3 G, the microwave power was 2 mW, and the frequency was 9.378 GHz. Observed g-values are found as $g = h\nu/\mu_B H_0$, where h is Planck's constant, μ_B is the Bohr magneton, ν is the operating frequency, and H_0 is the applied magnetic field value used to observe the EPR feature. The solvent was 2Me-THF, and the spectra were recorded at 20 K. The spectra were corrected for the cavity background measured for a sample of 2Me-THF.

Results and Discussion

The purpose of this study is to investigate if and how the photophysical properties of a D−B−A system are influenced by the spin state of a remote acceptor. Furthermore, the electronic structure of the bridge unit varies in the series of D−B−A systems, and this is expected to have a marked influence on the electronic communication between the donor and acceptor. To this end, we will compare the photophysics of a series of low-spin iron(III) porphyrin complexes (Zn(Im)P−RB−$Fe(Im)_2P^+$) with the corresponding high-spin iron(III) porphyrin complexes (ZnP−RB−Fe(Cl)P) and discuss the differences (Figure 1). This section will be organized as follows: First, EPR and UV/vis measurements that confirm that the spin state of the iron porphyrin changes from high- to low-spin by introducing imidazole are presented. Second, the total quenching efficiencies for the excited states of the zinc porphyrin donors based on steady-state and time-resolved fluorescence measurements are presented. Here, we show that the low-spin iron(III) porphyrin complexes behaves quite differently from the corresponding high-spin iron(III) porphyrin complexes. Next, we demonstrate that increased intersystem crossing previously observed as the dominating deactivation pathway for the singlet excited zinc porphyrin in the high-spin complexes[14] is only a minor contribution to the quenching of the low-spin iron(III) porphyrin complexes. Finally, we show that the quenching in the low-spin iron(III) porphyrin complexes is dominated by

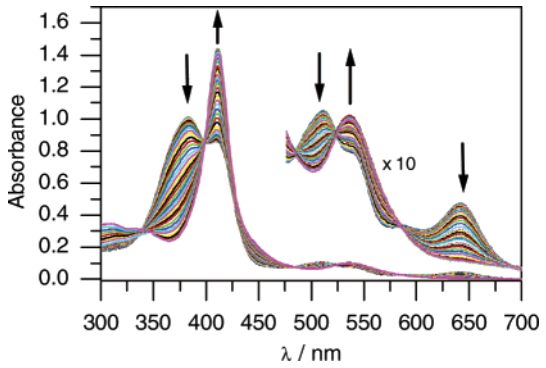

Figure 2. Spectrophotometric titration on FeP (~10 μM) with imidazole. The arrows indicate an increasing amount of imidazole (0 → 0.2 M). Solvent 2Me-THF.

electron transfer in contrast to the deactivation in the high-spin complexes. A corresponding set of measurements using the related free-base porphyrin donor showed similar results. Because these results just confirm the observations made with the zinc porphyrin donor, they were omitted from this Article.

Steady-State Absorption, Emission, and Spin-State Characterization. Because the purpose of this study is to investigate the effect of the acceptor spin state on the relative rates of the possible deactivation pathways in a D−B−A system, a tool to change this spin state is essential. Ligand-field strength, one of the major factors determining the ground-state electronic configurations of iron(III) porphyrins, has been recognized as an efficient and reliable tool to access different spin states of ferric porphyrins. Addition of a very strong-field ligand, such as imidazole, to high-spin ferric porphyrin complexes can be regarded as a classic way to obtain the corresponding low-spin complexes.[15] In Figure 2, a spectrophotometric titration on Fe(Cl)P in 2Me-THF with imidazole is shown. The presence of several well-defined isosbestic points indicates that two species are present − Fe(Cl)P[27] and $Fe(Im)_2P^+$. Moreover, analyses of binding isotherms[26] (not shown) confer that two imidazole ligands coordinate to FeP in accordance to what has been shown for tetraphenyl and octaethyl Fe(III) porphyrins.[15]

The EPR spectra of Fe(Cl)P and $Fe(Im)_2P^+$ show distinct differences in accordance with a change in spin state of the iron center (Figure S1, Supporting Information). The spectrum of Fe(Cl)P in 2Me-THF clearly resembles that of a high-spin ($S = {}^5/_2$) Fe(III) species, showing a high-intense axial symmetry signal with a g-value around 6.0 and a smaller signal with $g = 2.0$.[28] Such a signal is typical for a five-coordinated ferric compound with a moderate-field ligand such as a halide[15] and is essentially identical to spectra found for tetraphenyl and methyl-substituted tetraphenyl iron(III) porphyrins.[29] Adding the strong-field ligand imidazole to the 2Me-THF solution of Fe(Cl)P accomplishes a change in the spin state, from the high-spin to the low-spin ($S = {}^1/_2$), of the ferric complex as can be seen in the EPR spectrum. The EPR spectrum of $Fe(Im)_2P^+$ in 2Me-THF shows g-values of 2.8, 2.4, and 1.6. This rhombic spectrum is in agreement with a similar bis-(*N*-methyl imidazole) octaethyl tetraphenyl iron(III) porphyrin and is typical of low-spin Fe(III) porphyrin complexes.[30] Although the information about the actual structure of the Fe(Cl)P complex is not conclusive,[27] the ground-state electronic absorption and EPR measurements reported above clearly show that Fe(Cl)P in 2Me-THF exists as a high-spin complex provided no imidazole is added. The measurement also shows that addition of imidazole to the 2Me-THF solution of the high-spin ferric complex efficiently converts it to a low-spin $Fe(Im)_2P^+$ complex. The same results according to UV/vis measurements are obtained for the other two solvents used in this study (CH_2Cl_2, DMF).[31] Therefore, although Fe(Cl)P might exist as differently coordinated species due to solvation and solvent coordination, neither of the solvents used in this study have sufficiently high ligand-field strength to cause a change in the spin state of the ferric porphyrin from high- to low-spin.

In Figure 3, the absorption spectra of the low-spin iron(III) porphyrin complex Zn(Im)P−NB−$Fe(Im)_2P^+$ and of the high-spin iron(III) porphyrin complex ZnP−NB−Fe(Cl)P are shown together with the donor reference compounds, Zn(Im)P−NB and ZnP−NB, and the acceptors, Fe(Cl)P and $Fe(Im)_2P^+$. It is possible to resolve the dimer spectrum into the reference and the acceptor spectra, indicating that we have electronically separate chromophores. Introducing imidazole red-shifts and narrows the spectrum, indicating a more symmetric porphyrin because the central iron atom changes from five-coordinated to six-coordinated.[15] In addition, the peak at 650 nm which is characteristic for a high-spin iron(III) porphyrin disappears when switching to a low-spin iron(III) porphyrin (Figure 2).

Comparing the steady-state fluorescence spectra of the high- and low-spin complexes immediately indicates some important differences (Figure 3). Because the iron(III) porphyrin is nonfluorescent in both of its spin states, only the ZnP emission is detected. The fluorescence of ZnP shows the expected red-shift and a slight change in shape due to imidazole coordination. The important difference, though, is seen when comparing the series of different bridging chromophores. The quenching is clearly due to introduction of the acceptor unit in all cases, but while the high-spin complexes all show a high degree of quenching the low-spin series shows a much larger variation among the members of the series. Furthermore, as will be shown quantitatively below, the small quenching observed in Zn(Im)P−OB−$Fe(Im)_2P^+$ is entirely due to singlet energy transfer Zn(Im)P → $Fe(Im)_2P^+$. These differences − yet only indications − will be shown to be due to different quenching mechanisms for the low- and high-spin complexes.

Total Quenching Efficiencies. The fluorescence lifetimes (τ) of the molecules measured by single photon counting and the total quenching efficiencies (E_{DBA}) are presented in Table 1. To calculate $E_{DBA} = 1 - \tau_{DBA}/\tau_{DB}$, the decay traces of the D−B (τ_{DB}) and the D−B−A (τ_{DBA}) compounds were recorded while observing at the maximum emission wavelength. The decays were fitted to biexponential expressions, and the second component was a long-lived species (~1 ns, most likely traces of zinc porphyrin dimers) with a small preexponential factor

(27) In the following text, the abbreviation Fe(Cl)P is used to denote a high-spin ferric porphyrin acceptor, irrespective of its actual composition and structure. Although always in the high-spin state, the coordination sphere of iron(III) will vary between the various solvents used due to their different solvation and coordination abilities.

(28) Palmer, G. In *Iron Porphyins. Part II*; Lever, A. B. P., Gray, H. B., Eds.; Addison-Wesley Publishing Co.: Reading, MA, 1983; pp 43−88.

(29) Manso, C.; Neri, C. R.; Vidoto, E. A.; Sacco, H. C.; Ciuffi, K. J.; Iwamoto, L. S.; Iamamoto, Y.; Nascimento, O. R.; Serra, O. A. *J. Inorg. Biochem.* **1999**, *73*, 85−92.

(30) Ogura, H.; Yatsunyk, L.; Medforth, C. J.; Smith, K. M.; Barkigia, R. M.; Renner, M. W.; Melamed, D.; Walker, F. A. *J. Am. Chem. Soc.* **2001**, *123*, 6564−6578.

(31) Gouterman, M. In *Iron Porphyins. Part III*; Lever, A. B. P., Gray, H. B., Eds.; Addison-Wesley Publishing Co.: Reading, MA, 1983; pp 69−74.

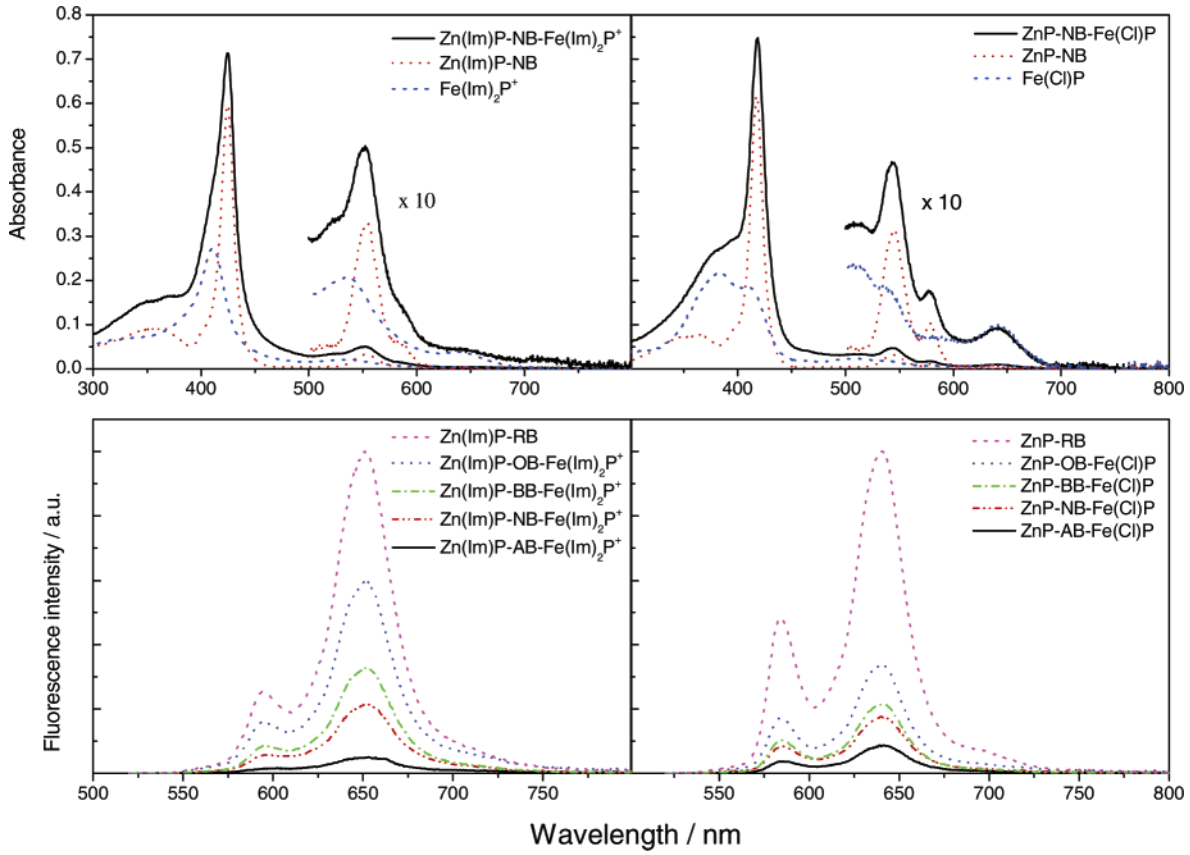

Figure 3. Upper: Absorption spectra. Lower: Emission spectra. Solvent 2Me-THF.

Table 1. Fluorescence Lifetimes of the Molecules (τ) and the Total Quenching Efficiencies (E_{DBA}) in 2Me-THF at Room Temperature

sample	τ (ps)	E_{DBA}[a] (%)	sample	τ (ps)	E_{DBA}[a] (%)
ZnP	1480		Zn(Im)P	1347	
ZnP−AB−Fe(Cl)P	119	91 ± 1	Zn(Im)P−AB−Fe(Im)$_2$P$^+$	57	95 ± 1
ZnP−AB	1356		Zn(Im)P−AB	1092	
ZnP−NB−Fe(Cl)P	262	81 ± 2	Zn(Im)P−NB−Fe(Im)$_2$P$^+$	345	73 ± 2
ZnP−NB	1389		Zn(Im)P−NB	1268	
ZnP−BB−Fe(Cl)P	303	78 ± 2	Zn(Im)P−BB−Fe(Im)$_2$P$^+$	519	58 ± 4
ZnP−BB	1390		Zn(Im)P−BB	1243	
ZnP−OB−Fe(Cl)P	486	67 ± 3	Zn(Im)P−OB−Fe(Im)$_2$P$^+$	1007	23 ± 8
ZnP−OB	1465		Zn(Im)P−OB	1311	

[a] The error margins for E_{DBA} are based on an estimated lifetime variation of ±5% (χ^2 < 1.4).

(less than 3%). Nevertheless, the long-lived species has a pronounced impact on the steady-state emission spectra, and this makes the efficiencies calculated from time-resolved more reliable than those estimated from steady-state measurements.

The general trend observed from the steady-state measurements prevails; the degree of quenching increases down the series of bridges, OB < BB < NB < AB. Furthermore, the different bridges have a larger effect on the quenching efficiencies for the imidazole complexed series than in the high-spin cases. This, again, indicates different mechanisms for quenching in the high- and low-spin complexes.

Nanosecond transient absorption was performed to study how the paramagnetic iron(III) porphyrin acceptor influences the intersystem crossing rate in the donor porphyrin. In Figure 4, the transient absorption traces of the excited zinc porphyrin triplet state − dimer and reference substances − are shown together with the expected traces, which are simulated assuming the intersystem crossing rate constants of the dimer (D−B−A), k_{isc}, and reference substance (D−B), k_{isc}^0, to be equal. Previously, we have shown that the high-spin iron(III) porphyrin enhances the intersystem crossing rate in the donor porphyrin.[14] In the low-spin iron(III) porphyrin systems, the intersystem crossing rate in the donor porphyrin is not enhanced. To reach a quantitative result, k_{isc} and k_{isc}^0, respectively, are compared. The quantum yields for intersystem crossing and fluorescence in the absence of the acceptor (i.e., for the reference substances) are given by:

$$\Phi_{isc}^{\ 0} = k_{isc}^{\ 0} \cdot \tau_{DB} \qquad \Phi_{f}^{\ 0} = k_{f}^{\ 0} \cdot \tau_{DB} \tag{1}$$

where k_f^0 and τ_{DB} are the rate constant for fluorescence and singlet lifetime of the reference substance, respectively. Likewise, the quantum yields for intersystem crossing and fluorescence in the presence of the acceptor (i.e., for the dimers) are given by:

$$\Phi_{isc} = k_{isc} \cdot \tau_{DBA} \qquad \Phi_{f} = k_{f} \cdot \tau_{DBA} \tag{2}$$

where k_f and τ_{DBA} are the rate constant for fluorescence and

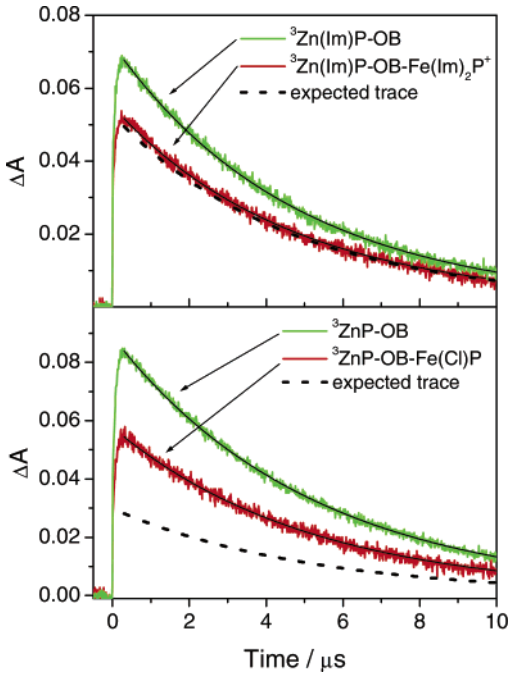

Figure 4. Kinetic traces (at 470 nm where ^{3}ZnP* has a maximum absorption) of dimer and reference substances for the low-spin acceptor (top diagram) and for the high-spin acceptor (bottom diagram). The expected traces for the dimers using the observed quenching rate constants and assuming $k_{isc}^0 = k_{isc}$ are shown with dashed lines. The black curves are monoexponential fittings corresponding to 5 μs. Solvent 2Me-THF.

lifetime of the dimer, respectively. Now, because the absorption spectrum (Figure 3) of the donor part (ZnP) is unaffected by appending the acceptor (FeP), it can be concluded that the radiative rate constants are equal for the donor fluorescence, that is, $k_f = k_f^0$. By combining eqs 1 and 2, the ratio of the rate constants for intersystem crossing is given by:

$$\frac{k_{isc}}{k_{isc}^0} = \frac{\Phi_{isc}/\Phi_{isc}^0}{\Phi_f/\Phi_f^0} = \frac{\Delta A_{DBA}/\Delta A_{DB}}{\tau_{DBA}/\tau_{DB}} \qquad (3)$$

The right-hand side of eq 3 needs further comments. ΔA_{DBA} and ΔA_{DB} are the measured maximum triplet absorption of the donor in the dimer and reference substance estimated from the nanosecond transient absorption trace at 470 nm (ZnP and Zn(Im)P). In other words, we are measuring the ZnP triplet formation with nanosecond transient absorption to estimate the ratio k_{isc}/k_{isc}^0 (eq 3). The values of ΔA_{DBA} and ΔA_{DB} are measured at "time zero"; however, as the triplet lifetimes of the reference and dimer substances (vide infra) are equal, the ratio between ΔA_{DBA} and ΔA_{DB} can be calculated at any time. From the ΔA values, the k_{isc}/k_{isc}^0 ratio is calculated (eq 3) using the measured singlet lifetimes (τ_{DBA} and τ_{DB}) in Table 1. The ratios between the intersystem crossing rate constants (eq 3) are 2.0 for ZnP−OB−Fe(Cl)P and 1.0 for Zn(Im)P−OB−Fe(Im)$_2$P$^+$. These measurements show that while intersystem crossing in the high-spin complexes is significantly enhanced the low-spin complexes have "normal" intersystem crossing rates and, consequently, the quenching of the singlet excited donor porphyrin must be caused by different processes in the two cases. In Figure 4, we have visualized the differences between the high- and low-spin complexes by indicating how the D−B−A trace would look if $k_{isc}/k_{isc}^0 = 1$, that is, no enhancement of the intersystem crossing rate (dashed line "expected trace"). For the high-spin complex (bottom spectra), the measured ΔA_{DBA} is larger than the "expected trace"; that is, the intersystem crossing rate is enhanced. On the other hand, the ΔA_{DBA} for the low-spin complex (top spectra) is at the same absolute ΔA-value as the expected trace; that is, there is no enhancement of the intersystem crossing rate. The ΔA_{DBA} values for the π-bridged systems are more difficult to analyze quantitatively than those for the OB-bridged system, due to donor triplet state quenching in these cases (vide infra). Nevertheless, the qualitative difference between the low- and high-spin systems seems to hold.

The triplet lifetimes of ZnP−OB, ZnP−OB−Fe(Cl)P, Zn(Im)P−OB, and Zn(Im)P−OB−Fe(Im)$_2$P$^+$ are all approximately the same (~5 μs), indicating that there is no triplet energy transfer from the donor to the acceptor for the OB-bridged systems.[14,32] At first sight, the uniform 5 μs triplet lifetime of the OB-bridged systems, which seems to be independent of the spin state of the acceptor, appears to be puzzling. However, for the zinc porphyrin used in this study, that is, a 5,15-diphenyl-2,3,7,8,12,13,17,18-octalkyl-substituted porphyrin, it has been shown that the triplet lifetime is many orders of magnitude shorter than for the corresponding tetraphenyl or octaalkyl porphyrins.[12] This is due to a conformational relaxation that leads to a nonplanar distortion of the porphyrin macrocycle in the excited triplet state.[33] This leads to a dramatic shortening of the triplet lifetime, and the distortion was shown to be thermally activated and consequently the lifetime is strongly temperature dependent. This might be the reason for not observing an enhancement of the intersystem crossing process ($T_1 \rightarrow S_0$) from the excited triplet to the ground state; the excited state is already heavily quenched by the conformational distortion, and the much smaller influence from the spin state of the acceptor is not possible to observe.

Femtosecond transient absorption was primarily performed to detect the ZnP radical cation (ZnP$^{\bullet+}$) which is one of the products resulting from intramolecular electron transfer. It would be satisfying if signatures of the FeP radical also could be detected, but they are probably too weak and/or broad and therefore hidden among the other absorbing species in the transient absorption spectra, which makes the assignment difficult. As an example, the transient absorption spectra of the low-spin complex (Zn(Im)P−BB−Fe(Im)$_2$P$^+$), the high-spin complex (ZnP−BB−Fe(Cl)P), and the corresponding reference substances (Zn(Im)P−BB and ZnP−BB) recorded at 1 ns delay time are shown in Figure 5. The strongest triplet absorption (^{3}ZnP*) is centered around 470 nm, and the singlet absorption (^{1}ZnP*) is centered around 500 nm.[12,26,34−36] At 1 ns delay time, ^{3}ZnP* absorption dominates the spectra between 450 and 520 nm for the reference and high-spin complex but is significantly weaker for the low-spin complex. Larger ΔA values for the high-spin complexes around 470 nm indicate that more triplets are formed, supporting the conclusion of enhanced intersystem

(32) Andréasson, J.; Kyrychenko, A.; Mårtensson, J.; Albinsson, B. *Photochem. Photobiol. Sci.* **2002**, *1*, 111−119.
(33) Kyrychenko, A.; Andréasson, J.; Mårtensson, J.; Albinsson, B. *J. Phys. Chem. B* **2002**, *106*, 12613−12622.
(34) Imahori, H.; Guldi, D. M.; Tamaki, K.; Yoshida, Y.; Luo, C.; Sakata, Y.; Fukuzumi, S. *J. Am. Chem. Soc.* **2001**, *123*, 6617−6628.
(35) Brun, A. M.; Harriman, A.; Heitz, V.; Sauvage, J. P. *J. Am. Chem. Soc.* **1991**, *113*, 8657−8663.
(36) Rodriguez, J.; Kirmaier, C.; Holten, D. *J. Am. Chem. Soc.* **1989**, *111*, 6500−6506.

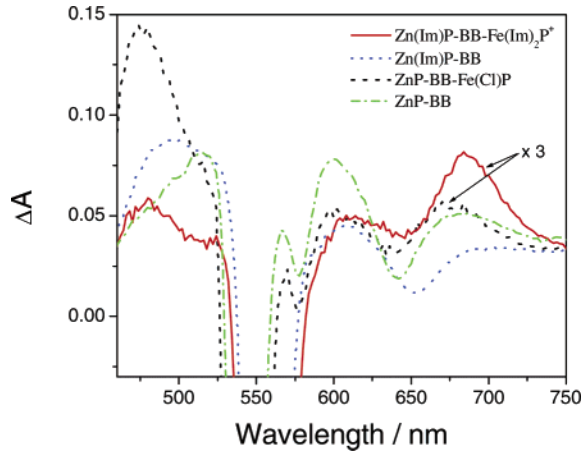

Figure 5. Transient absorption spectra at 1 ns delay time. The spectra of ZnP−BB−Fe(Cl)P and Zn(Im)P−BB−Fe(Im)$_2$P$^+$ are enlarged 3 times to make them comparable to the reference spectra. Solvent 2Me-THF.

crossing in the high-spin complexes. Furthermore, in the low-spin complex spectrum, a distinct peak around 680 nm is evident, which is assigned to ZnP$^{\bullet+}$.[26,37,38] In contrast, in the high-spin complex spectrum, no distinct peak around 680 nm is found, and its spectrum is interpreted as broad overlapping ^{1}ZnP* and ^{3}ZnP* bands with negative contributions from stimulated emission at 580 and 640 nm (emission maxima of the high-spin complex).

In Figure 6, transient absorption decay traces monitored at 680 nm are shown for the high- and low-spin complexes of the four different bridged systems. The fast component that dominates the decays at short times (<2 ps) is due to the relaxation of the FeP excited state which is directly excited by the laser.[14] The donor, ZnP, cannot be excited exclusively, and with 545 nm excitation 20−50% (solvent and coordination species dependent) of the incident light excites FeP.

At longer times, the differences between the high- and low-spin complexes are striking; for example, for ZnP−NB−Fe(Cl)P, a monotonic decaying transient is observed, while for the Zn(Im)P−NB−Fe(Im)$_2$P$^+$ complex, the transient absorption at 680 nm builds up before it decays. The decays at longer decay times at 680 nm of the high-spin complexes can accurately be fitted to the same lifetimes as the fluorescence decays of the dimers. Further, the low-spin complexes with fully conjugated bridges (complexes with AB-, NB-, and BB-bridges) exhibit a build-up time followed by a slower decay at 680 nm. The build-up times in the transients of the low-spin complexes Zn(Im)P−NB−Fe(Im)$_2$P$^+$ and Zn(Im)P−BB−Fe(Im)$_2$P$^+$ are the same as the fluorescence lifetimes; that is, the formation of ZnP$^{\bullet+}$ is directly linked to the decay of the singlet excited ZnP. In contrast, the rise time in the transient of Zn(Im)P−AB−Fe(Im)$_2$P$^+$ is significantly faster (10−20 ps) than the fluorescent lifetime (57 ps), which might reflect an equilibrium situation between the excited ZnP and the intermediate charge-separated species, Zn(Im)P$^{\bullet+}$−AB$^{\bullet-}$−Fe(Im)$_2$P$^+$. The potential competition between a stepwise and direct electron-transfer mechanism is presently being studied in the related systems with a gold(III) porphyrin acceptor.[39] In addition, the low-spin OB-bridged complex, Zn(Im)P−OB−Fe(Im)$_2$P$^+$, shows no build-up time at 680 nm but only a decay on the nanosecond time-scale. Transient absorption traces at 500 nm were also recorded for all dimers. By and large, the lifetime of the singlet excited ZnP plus a longer lifetime, presumably due to ZnP triplet decay, could be fitted to the data.

In summary, we have detected the zinc porphyrin radical cation, ZnP$^{\bullet+}$, formed by electron transfer in the low-spin complexes with the π-conjugated bridges (AB, NB, BB). This is in marked contrast to the corresponding high-spin complexes where enhanced intersystem crossing induced by the remote FeP(Cl) is the main source of ^{1}ZnP* quenching. As a result, simply adding imidazole switches the present D−B−A system from a situation where the excitation energy is localized on the donor (increased intersystem crossing) to a system that performs electron transfer on the picosecond time-scale. Because the low-spin complex with the OB-bridge does not show the ZnP$^{\bullet+}$ absorption peak, and as no enhancement of intersystem crossing is detected by the nanosecond transient absorption measurements, we can conclude that singlet energy transfer is the only feasible deactivation channel. It is also reassuring that the estimated Förster rate constant is of the same order as the quenching rate constant in this case (vide infra). In this respect, these findings are in line with the results obtained before with similar systems bearing a gold(III) porphyrin acceptor (ZnP−RB−AuP$^+$).[13]

Rate Constants. To quantitatively compare the different systems, the rate of donor fluorescence quenching is calculated (eq 4) and collected in Table 2. The relevant energy levels and potential relaxation pathways for the ZnP/Fe(III)P systems are also shown in Figure 7. The total quenching rate constant, k_q, is equal to the sum of all additional processes that contributes to the increased deactivation rate of the donor, and in eq 4 this has been expressed as the sum of rate constants for the Förster energy transfer ($k_{Förster}$), the increased intersystem crossing ($k_{isc} - k_{isc}^0$), and a rest-term (k_{rest}).

$$k_q = \frac{1}{\tau_{DBA}} - \frac{1}{\tau_{DB}} = k_{Förster} + (k_{isc} - k_{isc}^0) + k_{rest} \qquad (4)$$

Please observe that k_{rest} represents different deactivation processes − electron transfer or enhanced intersystem crossing − depending on which system is discussed. The rate constant for intersystem crossing in the reference compound is calculated from eq 1 where the intersystem crossing quantum yield is assumed to be equal to the value for zinc tetraphenylporphyrin, 0.90.[40] The rate constant for intersystem crossing in the dimer compounds (k_{isc}), with the OB-bridge, is calculated from the measured ratio k_{isc}/k_{isc}^0 (eq 3). The enhancement of the intersystem crossing rate ($S_1 \rightarrow T_1$) of the ZnP donor is probably influenced by the bridge in the same fashion as has been observed for electron transfer and excitation energy transfer for similar systems.[10,13] As a consequence, k_{isc} is expected to increase going from OB, BB, NB to the AB-bridge. However, ΔA_{DBA} values for the π-bridged systems are more difficult to analyze quantitatively due to donor triplet state quenching in these cases. Therefore, we estimate k_{isc} for the π-bridged systems

(37) Imahori, H.; Hagiwara, K.; Aoki, M.; Akiyama, T.; Taniguchi, S.; Okada, T.; Shirakawa, M.; Sakata, Y. *J. Am. Chem. Soc.* **1996**, *118*, 11771−11782.
(38) Chosrowjan, H.; Tanigichi, S.; Okada, T.; Takagi, S.; Arai, T.; Tokumaru, K. *Chem. Phys. Lett.* **1995**, *242*, 644−649.
(39) Winters, M.; Pettersson, K.; Mårtensson, J.; Albinsson, B., manuscript in preparation.
(40) Harriman, A.; Porter, G.; Wilowska, A. *J. Chem. Soc., Faraday Trans. 2* **1983**, *79*, 807−816.

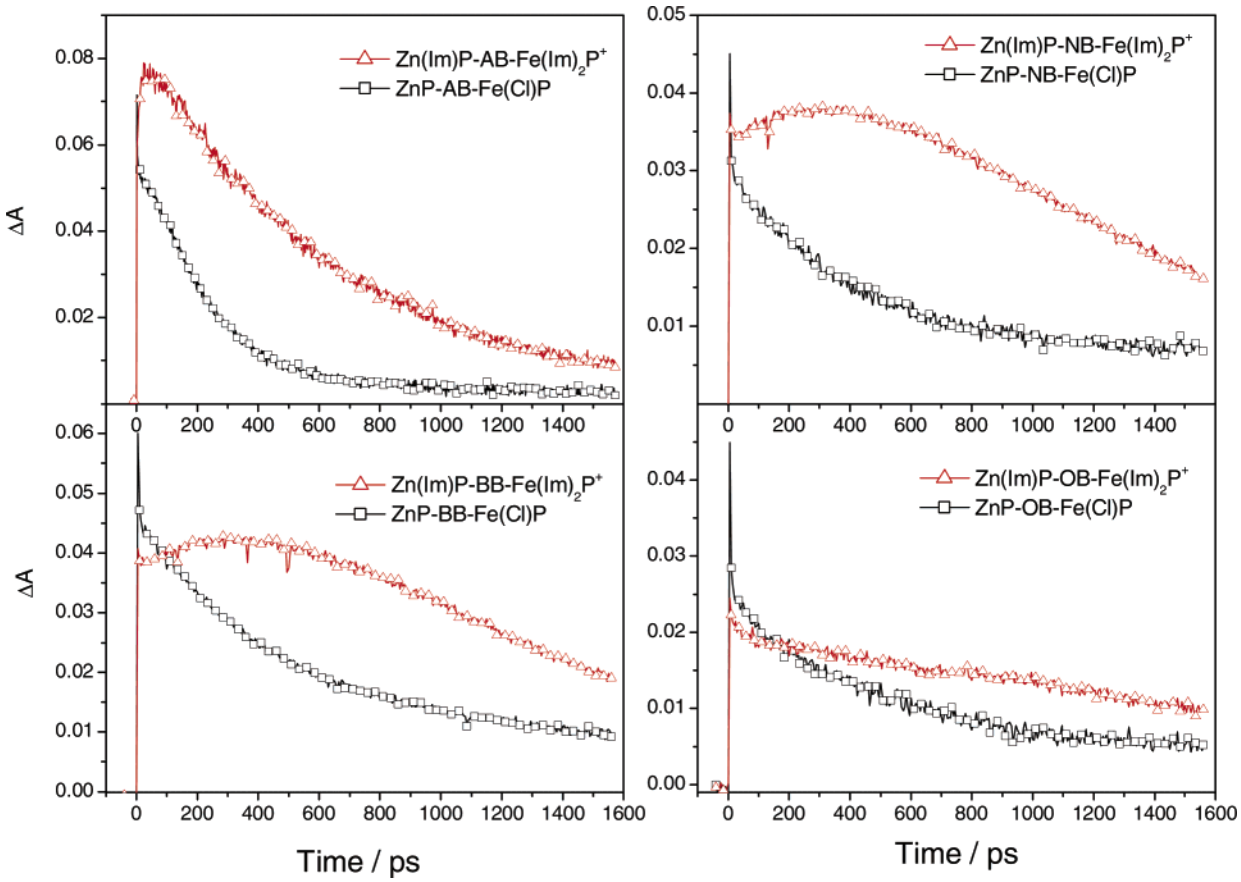

Figure 6. Kinetic traces of the dimers with a low-spin acceptor (△) and a high-spin acceptor (□) at 680 nm where $ZnP^{\bullet+}$ and $^1ZnP^*$ dominate the absorption. Solvent 2Me-THF.

Table 2. Total Quenching Rate Constant (k_q), Rate Constants for Intersystem Crossing (ISC) in the Absence (k_{isc}^0) and in the Presence of the FeP Acceptor (k_{isc}), Calculated Förster Rate Constant ($k_{Förster}$), and Rest-Term, k_{rest}[a]

sample	[b] k_q (ns^{-1})	[c] k_{isc}^0 (ns^{-1})	[d] k_{isc} (ns^{-1})	$k_{Förster}$ (ns^{-1})	[e] k_{rest} (ns^{-1})	dominating quenching process
ZnP−AB−Fe(Cl)P	7.7 ± 0.5	0.66 ± 0.05	≥1.3 ± 0.1	0.5 ± 0.1	≤6.5 ± 0.5	ISC/EET
ZnP−NB−Fe(Cl)P	3.1 ± 0.2	0.65 ± 0.05	≥1.3 ± 0.1	0.5 ± 0.1	≤2.0 ± 0.2	ISC/EET
ZnP−BB−Fe(Cl)P	2.6 ± 0.2	0.65 ± 0.05	≥1.3 ± 0.1	0.5 ± 0.1	≤1.5 ± 0.2	ISC/EET
ZnP−OB−Fe(Cl)P	1.4 ± 0.2	0.61 ± 0.05	1.2 ± 0.1	0.5 ± 0.1	0.3 ± 0.2	ISC/EET
$Zn(Im)P-AB-Fe(Im)_2P^+$	17 ± 1.0	0.82 ± 0.05	0.8 ± 0.05	0.2 ± 0.04	16 ± 1.0	ET
$Zn(Im)P-NB-Fe(Im)_2P^+$	2.1 ± 0.2	0.71 ± 0.05	0.7 ± 0.05	0.2 ± 0.04	1.9 ± 0.2	ET
$Zn(Im)P-BB-Fe(Im)_2P^+$	1.1 ± 0.2	0.72 ± 0.05	0.7 ± 0.05	0.2 ± 0.04	0.9 ± 0.2	ET
$Zn(Im)P-OB-Fe(Im)_2P^+$	0.23 ± 0.09	0.69 ± 0.05	0.7 ± 0.05	0.2 ± 0.04	0	EET

[a] The dominating quenching process is suggested in the last column, that is, ISC (enhancement of the ISC rate as compared to the reference substance), electron transfer (ET), or excitation energy transfer (EET). Solvent 2Me-THF. The error margins are calculated using an estimated lifetime variation of ±5%. [b] Equation 4. [c] Equation 1. [d] The ratio k_{isc}/k_{isc}^0 is measured for the OB-bridged systems and estimated for the π-bridged systems; see text for details. [e] $k_{rest} = k_q - (k_{isc} - k_{isc}^0) - k_{Förster}$. Please observe that k_{rest} accounts for different deactivation processes for different systems; see text for details.

to be of the same magnitude or larger than k_{isc} for the OB-bridged system (Table 2).

The Förster energy-transfer rate constant, $k_{Förster}$, is calculated from the structural and spectroscopic properties of the D−B−A systems.[14] It is seen in Table 2 that energy transfer dominates the donor quenching in $Zn(Im)P-OB-Fe(Im)_2P^+$ while for the other low-spin complexes with π-conjugated bridges (AB, NB, BB) the rest-term dominates (eq 4). Because the transient absorption measurements clearly show that electron transfer is the most important process connected to the excited-state relaxation in the low-spin complexes, we interpret this rest-term to be dominated by electron transfer.

The last column of Table 2 gives a summary of the dominating deactivation pathways. For the high-spin complexes, the increased intersystem crossing and energy-transfer terms both contribute significantly. This is most obvious for ZnP−OB−Fe(Cl)P, where the enhanced intersystem crossing and the estimated energy-transfer rates contribute equally to the measured donor quenching. The situation is more complicated when interpreting the π-bridged high-spin complexes because in these cases the rest-term makes a significant contribution. However, from studies on similarly bridged systems, we know that the rate of excitation energy transfer is strongly affected by the electronic structure of the bridging chromophore.[10,11,13] This is a consequence of the bridge-mediated electronic coupling which causes both energy transfer and potentially the intersystem crossing to be much faster. In the corresponding ZnP−RB−H_2P systems, we found that the bridge-mediated energy transfer

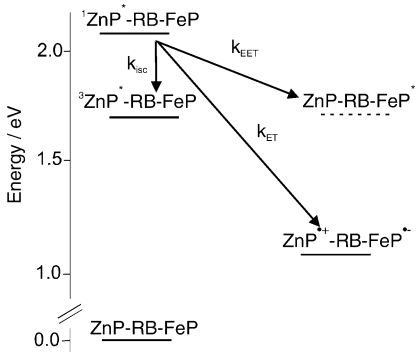

Figure 7. Energy level diagram for ZnP−RB−FeP in 2Me-THF. The energy of the lowest FeP excited state is not experimentally determined and is therefore indicated by a dashed line.

increased in the series BB < NB < AB, in accordance with the trend observed for the rest-term found in this study. Moreover, from the femtosecond transient absorption measurements, we can rule out electron transfer to be responsible for the rest-term in the high-spin complexes.

Electron Transfer versus Intersystem Crossing. According to the Marcus theory, the rate constant for diabatic electron transfer in the high-temperature limit is:

$$k_{ET} = \sqrt{\frac{\pi}{\hbar^2 \lambda k_B T}} |V|^2 \exp\left[-\frac{(\Delta G^\circ + \lambda)^2}{4\lambda k_B T}\right] \qquad (5)$$

where k_B is the Boltzmann constant, T is the temperature, V is the electronic coupling, and λ is the total reorganization energy. The thermodynamic driving force ΔG° and the reorganization energy λ can be calculated using redox potentials for the interacting species together with solvent dielectrical properties and donor/acceptor radii.[41−44]

$$\Delta G^0 = e(E_{ox} - E_{red}) - E_{00} - \frac{e^2}{4\pi\epsilon_0\epsilon_s R_{DA}} + \frac{e^2}{4\pi\epsilon_0}\left(\frac{1}{\epsilon_s} - \frac{1}{\epsilon_s^{ref}}\right)\left(\frac{1}{2R_D} + \frac{1}{2R_A}\right) \qquad (6)$$

$$\lambda = \lambda_i + \lambda_s = \lambda_i + \frac{e^2}{4\pi\epsilon_0}\left(\frac{1}{2R_D} + \frac{1}{2R_A} - \frac{1}{R_{DA}}\right)\left(\frac{1}{n^2} - \frac{1}{\epsilon_s}\right) \qquad (7)$$

Relevant numerical values for all parameters have been reported previously,[14] except for the reduction potential of $Fe(Im)_2P^+$ which is fairly difficult to accurately determine due to irreversible redox processes. However, by comparison to other ferric porphyrins where the reduction potentials for high- and low-spin complexes have been compared, it can safely be concluded that they are within 100 meV.[45,46] The same redox potentials are used for the high- and low-spin redox pairs; as a consequence, only the E_{00} shift changes the driving force between the high- and low-spin complexes. In Table 3, ΔG°, λ, and $\Delta G^\circ + \lambda$ are reported for three different solvents (2Me-THF, CH_2Cl_2, DMF), with the uncertainty of ±100 meV included for the low-spin complexes. As seen in Table 3 for the ZnP/Fe(Cl)P pair, the driving force is about 1 eV yielding an estimated barrier free electron-transfer reaction ($\Delta G^\circ + \lambda \approx 0$) in all three solvents (eq 5). For a barrier free electron-transfer reaction, a shift in the driving force by 100 meV up or down can solely result in a slower electron-transfer rate (by 60% with 1 eV reorganization energy). Because the opposite is observed, the driving force alone cannot explain the fact that electron transfer is more feasible in the low-spin complex, and according to eq 5 the observed rate increase must be caused by a larger electronic coupling, V. Of importance might be the changes in distortion from planarity of the porphyrin ring upon changing the coordination of the iron porphyrin. In going from a five-coordinated iron in Fe(Cl)P to a six-coordinated complex $Fe(Im)_2P^+$ with two axial ligands on opposite sides of the porphyrin ring, the changes in ring distortion are expected to be associated with alterations in both orbital symmetries and orbital energies.[47,48] Such variations could have a large effect on the electronic coupling between the acceptor and bridge units.[49] In addition, as compared to the out-of-plane five-coordinated system, an increased electronic coupling between the iron center and the rest of the D−B−A system is expected for the six-coordinated low-spin system where the iron atom is located in the plane of the porphyrin.[50] This may be of importance because the reduction of iron(III) porphyrins is suggested to take place on the iron center.[28,51,52] Portela et al. also report a much larger ET rate for their low-spin acceptor dimer (ZnP/FeP) as compared to a high-spin acceptor dimer and suggest that it is due to that the iron is in the porphyrin plane in the low-spin case and out-of-plane in the high-spin case.[20]

Table 3. Calculated Driving Forces (ΔG°) and Reorganization Energies (λ) in Different Solvents[a]

sample	solvent	ΔG° (eV)	λ (eV)	$\Delta G^\circ + \lambda$ (eV)
ZnP−RB−Fe(Cl)P	2Me-THF	−1.01	0.98	−0.03
ZnP−RB−Fe(Cl)P	CH_2Cl_2	−1.08	1.03	−0.05
ZnP−RB−Fe(Cl)P	DMF	−1.29	1.22	−0.07
$Zn(Im)P-RB-Fe(Im)_2P^+$	2Me-THF	−0.97 ± 0.1	0.98	0.01 ± 0.1
$Zn(Im)P-RB-Fe(Im)_2P^+$	CH_2Cl_2	−1.05 ± 0.1	1.03	−0.02 ± 0.1
$Zn(Im)P-RB-Fe(Im)_2P^+$	DMF	−1.29 ± 0.1	1.22	−0.07 ± 0.1

[a] Estimated uncertainties for the imidazole complexes; see text for details.

It is interesting to compare the electron-transfer rates for the present ZnP−RB−FeP^+ series with the corresponding series with gold(III) porphyrin as the acceptor, ZnP−RB−AuP^+.[13] With the ZnP/AuP redox couple, the driving force for electron transfer is significantly smaller ($\Delta G^\circ = -0.61$ eV in 2Me-THF). Nevertheless, the observed electron-transfer rates are similar to those reported here for the low-spin complexes. This again suggests that the electronic coupling rather than the thermodynamic driving force is the important factor that explains the

(41) Marcus, R. A. *Can. J. Chem.* **1959**, *37*, 155−163.
(42) Marcus, R. A. *J. Chem. Phys* **1965**, *43*, 679−701.
(43) Rehm, D.; Weller, A. *Ber. Bunsen-Ges. Phys. Chem.* **1969**, *73*, 834−839.
(44) Weller, A. *Z. Phys. Chem. NF* **1982**, *133*, 93−98.
(45) O'Brien, P.; Sweigart, D. A. *Inorg. Chem.* **1985**, *24*, 1405−1409.
(46) Doeff, M. M.; Sweigart, D. A.; O'Brien, P. *Inorg. Chem.* **1983**, *22*, 851−852.
(47) Barkigia, K. M.; Chantranupong, L.; Smith, K. M.; Fajer, J. *J. Am. Chem. Soc.* **1988**, *110*, 7566−7567.
(48) Poveda, L. A.; Ferro, V. R.; Garcia de la Vega, J. M.; Gonzalez-Jonte, R. H. *Phys. Chem. Chem. Phys.* **2000**, *2*, 4147−4156.
(49) Yang, S. I.; Seth, J.; Balasubramanian, T.; Kim, D.; Lindsey, J. S.; Holten, D.; Bocian, D. F. *J. Am. Chem. Soc.* **1999**, *121*, 4008−4018.
(50) Ghosh, A.; Halvorsen, I.; Nilsen, H. J.; Steene, E.; Wondimagegn, T.; Lie, R.; van Caemelbecke, E.; Guo, N.; Ou, Z.; Kadish, K. M. *J. Phys. Chem. B* **2001**, *105*, 8120−8124.
(51) Johansson, M. P.; Blomberg, M. R. A.; Sundholm, D.; Wikström, M. *Biochim. Biophys. Acta* **2002**, *1553*, 183−187.
(52) Goeff, H. M. In *Iron Porphyins. Part I*; Lever, A. B. P., Gray, H. B., Eds.; Addison-Wesley Publishing Co.: Reading, MA, 1983; pp 237−281.

difference between the high- and low-spin ferric complexes. The Zn(Im)P−RB−Fe(Im)$_2$P$^+$ and ZnP−RB−AuP$^+$ series also behave quite similar with respect to variation of the electron-transfer rates as a function of bridging chromophore. In both series, no electron transfer is observed for the bridges with broken π-conjugation (OB), and the rate increases as the energy gap between the relevant donor and bridge states decreases. This is perfectly in line with the superexchange model, but because this has been thoroughly discussed and quantitatively investigated in a previous paper, we will refrain from repeating it here.[13]

Concluding Remarks

By changing the spin state of the paramagnetic acceptor from high-spin ($S = {}^5/_2$) to low-spin ($S = {}^1/_2$), the deactivation of the excited donor porphyrin changes from enhanced intersystem crossing to electron transfer in the systems connected by fully π-conjugated bridges. Two opposing mechanisms are expected to cause this dramatic dependence on imidazole coordination. First, the magnitude of the acceptor spin angular momentum is decreased which causes the rate of triplet formation in the donor porphyrin to decrease to its normal rate. Second, the suggested change in structure of the acceptor porphyrin[47,48,50] turns it into a better electron acceptor due to larger electronic coupling to the rest of the system. Thus, larger electronic coupling and less competition from other deactivation processes turns a poor electron transducing D−B−A system into a good one. As observed before, when the bridge is not π-conjugated, electron transfer is not observed, and energy transfer is the dominating deactivation pathway for the low-spin OB-bridged system.

Acknowledgment. This work was supported by grants from the Swedish Research Council, the Knut and Alice Wallenberg Foundation, and the Hasselblad Foundation. We thank Dr. Angel J. Di Bilio for skillful assistance with recording of the EPR spectra.

Supporting Information Available: EPR spectra of Fe(Cl)P and Fe(Im)$_2$P$^+$ in 2Me-THF at 20 K. This material is available free of charge via the Internet at http://pubs.acs.org.

JA0370488